Electrically detected magnetic resonance using radio-frequency reflectometry

Author/Contributor:
Huebl, H.; Starrett, R. P.; McCamey, D. R.; Ferguson, A. J.; Willems van Beveren, Laurens Henry

Publication details:
Review of Scientific Instruments
v. 80
Chapter No. 11
pp. 114705-1-114705-4
0034-6748 (ISSN)

Publication Date:
2009

Publisher DOI:
http://dx.doi.org/10.1063/1.3258206

Electrically detected magnetic resonance using radio-frequency reflectometry

H. Huebl,[a] R. P. Starrett, D. R. McCamey,[b] A. J. Ferguson,[c] and L. H. Willems van Beveren

Australian Research Council Centre of Excellence for Quantum Computer Technology, School of Physics, The University of New South Wales, Sydney 2052, Australia

(Received 30 September 2009; accepted 13 October 2009; published online 11 November 2009)

The authors demonstrate readout of electrically detected magnetic resonance at radio frequencies by means of a *LCR* tank circuit. Applied to a silicon field-effect transistor at millikelvin temperatures, this method shows a 25-fold increased signal-to-noise ratio of the conduction band electron spin resonance and a higher operational bandwidth of >300 kHz compared to the kilohertz bandwidth of conventional readout techniques. This increase in temporal resolution provides a method for future direct observations of spin dynamics in the electrical device characteristics. © *2009 American Institute of Physics.* [doi:10.1063/1.3258206]

Spin resonance is commonly used to spectroscopically identify spin species in material systems, particular in semiconductors,[1] and it also allows spin dynamics to be studied using pulsed excitation techniques.[2] Although classical spin resonance has the ultimate detection bandwidth, as the signal is detected directly via the re-emission of microwave radiation, the technique is usually limited to large spin ensembles.[3] In order to investigate few[4] and ultimately a single spin[5–8] the spin information is transferred to a secondary quantity, such as charges or photons, which can be detected sensitively. Such direct electrical readout in electrically detected magnetic resonance (EDMR) is typically limited to the low bandwidths in the kilohertz regime. Therefore, coherent spin information can only be recovered from the long term electronic evolution of the sample after the microwave pulse.[9,10] The development of radio frequency (rf) detection schemes for single-electron transistor (SET) electrometry[11] has overcome the limitation of low bandwidths. This has been achieved by embedding the sample in a resonant *LCR* circuit which matches the probed resistance information to the impedance of the rf circuitry of 50 Ω, allowing the measurement of the sample resistance at high bandwidths.

In this letter we apply the *LCR* tank circuit developed for rf SETs to the detection of spin phenomena (in the following referred to as rfEDMR). We measure the rf reflectance of the *LCR* circuit as well as the low-frequency resistance of a metal-oxide-semiconductor field-effect transistor (MOSFET) and observe changes in both quantities under electron spin resonance (ESR). Furthermore, the temporal dependence of rfEDMR is studied and compared to conventional (low-frequency) EDMR demonstrating the high bandwidth of rfEDMR. This could in principle allow the direct investigation of coherently manipulated spin states, like Rabi oscillations as opposed to the reconstruction discussed in detail in Ref. 9. Additionally, in contrast to earlier, noncontact rf readout techniques,[12] the direct bias of the MOSFET channel with rf current in rfEMDR allows to investigate micron size or smaller devices.

Using a *LCR* resonant circuit for the detection of EDMR requires that the change in the device resistance, monitored at virtually dc (<10 kHz), can be detected at the resonance frequency f_{rf} of the *LCR* circuit, typically a few hundred megahertz. While this seems valid for high device mobilities, e.g., transport in the conduction band of Si,[13] systems where the transport is hopping mediated[14] may be an example where this method is not applicable. For a silicon MOSFET, the spin-to-charge conversion process originates from a difference in scattering amplitudes for randomly formed spin pairs in singlet and triplet configuration in the MOSFET channel, the relative contribution of which is changed under spin resonance conditions, leading to a change in the total conductance of the electron accumulation layer by $\Delta\sigma/\sigma \approx 10^{-4}$.[13,15,16] Incorporating this device as the resistive element in a *LCR* resonant circuit allows us to measure resistance changes via the magnitude of the absorption at f_{rf}.[11] This is conveniently measured in reflection, where the reflection coefficient Γ is determined by the impedance mismatch between the coaxial line and the *LCR* circuit. In EDMR spin resonance manifests in a change ΔR of the total device resistance R and for rfEDMR small changes in ΔR, close to the matching condition $|Z_{LCR}(f)| \approx 50\ \Omega$, will result in a change in $\Gamma \propto \Delta R$. Additionally, calibration of the rf reflectance can be obtained by measuring the dc device resistance simultaneously and assuming that it is independent of the probe frequency.[11] The resistance can then be accessed quantitatively using the rf circuit, retaining the benefit of the increased bandwidth.

The MOSFET [cf. Figure 1(a)] investigated is fabricated on natural bulk silicon with a phosphorus doping of $[\mathrm{P}] = 8 \times 10^{16}\ \mathrm{cm}^{-3}$ and has a 20 nm thick, high-quality SiO_2

[a]Author to whom correspondence should be addressed. Electronic mail: huebl@wmi.badw.de. Present address: Walther-Meissner-Institut, Bayerische Akademie der Wissenschaften, Garching, Germany.

[b]Present address: Department of Physics, University of Utah, 115 S 1400 E, Suite 201, Salt Lake City, Utah 84112-0830, USA.

[c]Present address: Cavendish Laboratory, JJ Thomson Avenue, Cambridge CB3 0HE, United Kingdom.

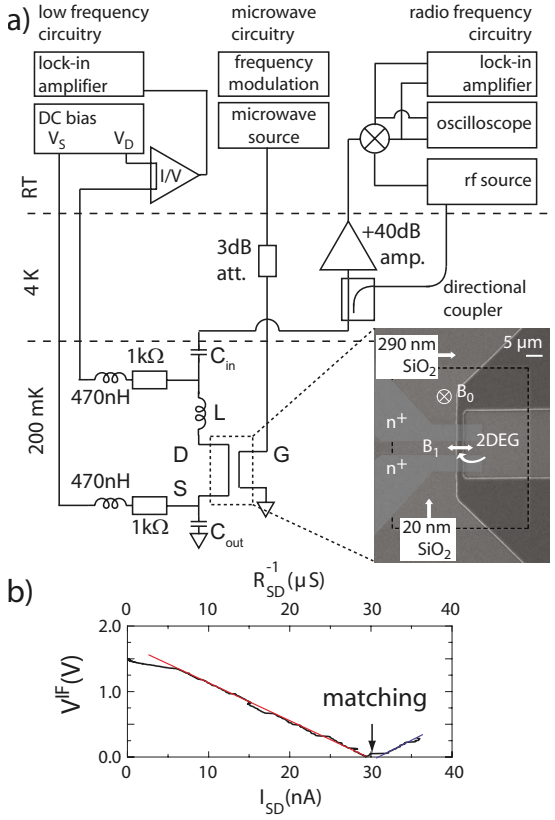

FIG. 1. (Color online) Panel (a) shows the EDMR detection setup including the low frequency, the microwave, and the rf circuitry. The inset shows a scanning electron micrograph of the silicon MOSFET. Panel (b) shows the calibration curve that translates the source-drain conductance/current (V_{SD} =1 mV) to the reflected rf signal amplitude after homodyning V_{IF}. At 30 nA a matching point is observed. The red and blue lines are guides to the eye and show a slope of −57.9 and 48 mV/nA, respectively.

gate oxide. Source and drain contacts are formed by indiffused phosphorus regions with $[P]=3\times10^{19}$ cm^{-3}.[15] A shorted strip line is used simultaneously as a gate electrode to accumulate electrons and as a local antenna to provide the microwave magnetic field B_1 which excites the spin transitions. The MOSFET is turned on by grounding the gate and applying a differential voltage across the source and drain contacts V_{SD}, commonly offset from the top gate potential V_G. The source drain current I_{SD} is measured by a current amplifier (SIM918). For the experiments shown here, the microwave frequency applied is $f_{MW}=37.9044$ GHz with a source power of 10 dBm. In order to employ phase-sensitive detection with a lock-in amplifier we modulate the frequency of the microwave sinusoidally with variable rate f_{mod} and a depth of 1.5 MHz equivalent to 0.2 mT magnetic field modulation.[15] The experiment is performed in a dilution refrigerator at ≈200–300 mK, which is inserted into a superconducting magnet to provide a static magnetic field B_0, oriented along the [001]-direction of the Si crystal and perpendicular to the sample surface. Additionally, B_0 is corrected for a constant offset, using the ^{31}P hyperfine split signature with a center of gravity g-factor of 1.9985 of a reference spectrum.[17] Figure 1(a) shows the dc and rf part of the electrical setup used for EDMR detection in this experiment. The *LCR* circuit is realized by a surface mount inductor (L=330 nH) on a printed circuit board located close to the source contact of the MOSFET. The capacitance (C

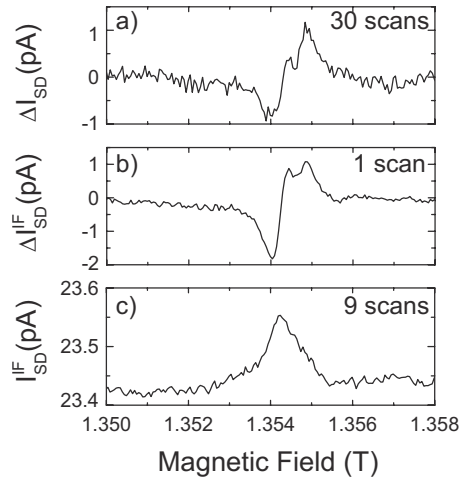

FIG. 2. EDMR using different detection schemes. Panel (a) shows the EDMR signal obtained by monitoring the lock-in amplified source drain current. Panel (b) shows the reflected rf signal from the *LCR* circuit using homodyne detection, lock-in amplification, and conversion to a current scale using Fig. 1(b) with a 25-fold increased signal to noise. Panel (c) shows the absolute (converted) current change, monitored directly by measuring V_{IF} with a storage oscilloscope.

≈500 fF) is given by the parasitic capacitance from source to drain and drain to the gate. The resistor R is formed by the source-to-drain resistance of the MOSFET. The resonance frequency of this circuit under matching conditions is 385.13 MHz defining the rf frequency f_{rf} used for rfEDMR. Additionally, C_{in} and C_{out}, each 100 pF, in combination with 1 kΩ NiCr resistors and 470 nH surface mount inductors form biasing tees, decoupling the rf and dc signals. The rf reflectometry is realized by sending a rf signal to a directional coupler (15 dB, at the 4 K stage) and amplifying the reflected signal with a Quinstar cold amplifier (T_N=3.1 K) also located at the 4 K stage. After demodulating the amplified reflected rf signal using a homodyne detection scheme, involving quadrature demodulation (AD8348) at room temperature, the resulting dc signal $V_{IF}\propto\Gamma$ is recorded by either a lock-in amplifier or by a digital storage oscilloscope (DSO).

In order to calibrate the rf detection setup, we record the source-drain current I_{SD} as well as the demodulated rf signal V_{IF} for $f_{rf}=385.13$ MHz as function of the top gate voltage V_G. Figure 1(b) shows V_{IF} as function of I_{SD} or $1/R_{SD}$ for a source-drain bias V_{SD}=1 mV. In the I_{SD} regime between 6 and 30 nA, we observe a linear relation of −57.9 mV/nA, which we use to convert V_{IF} into I_{SD}^{IF} and ΔI_{SD}^{IF}. The presence of a matching point in the response of the tank circuit is a particular advantage of rfEDMR because here $\Gamma\propto\Delta R$ which suppresses the finite I_{SD} intrinsically. In contrast, conventional EDMR generally suffers from the challenge of measuring a small resistance or current change on a relatively large current offset.

Figure 2 compares the different EDMR detection modes for a gate voltage V_g=0.64 V, a source-drain bias V_{SD} =1 mV resulting in I_{SD}=23.4 nA, close to matching of the *LCR* circuit. Panel (a) shows the lock-in detected source drain current ΔI_{SD} of a conventional EDMR spectrum acquired over a total of 30 magnetic field scans. Two resonant lines are observed, one at B_0=1.354 29 T corresponding to g=1.9997 in good agreement with the conduction band elec-

tron signal of the accumulation layer[17] and a second one at $B_0=1.354\ 74$ T ($g=1.999$) possibly originating from exchange coupled P donors.[18] Interestingly, the two hyperfine-split lines expected for isolated phosphorus donors in silicon are not present in this spectrum. Their absence appears to be related to the bias conditions of the MOSFET, as they are present for higher source-drain bias (50 mV) and lower V_G (0.3 V - not shown). This could be due to the trapping of electrons in a diamagnetic P^- state which is ESR inactive. This state is approx 2–3 meV below the conduction band and therefore the thermal excitation at low temperatures $\propto 200-300$ mK and the resulting slow escape rate could explain the absence of the lines,[19] whereas for high bias conditions an increased escape rate due to tunneling is expected. This effect, while interesting, is beyond the scope of this publication focusing on the high-bandwidth readout and will be discussed elsewhere.

Figure 2(b) shows the demodulated and lock-in amplified reflected rf signal, converted into an equivalent current using the calibration curve of Fig. 1(b) measured under the same conditions as in Fig. 2(a). This spectrum was obtained in a single magnetic field scan with an incident rf power of -55 dBm or ~ 0.4 mV at the input of the *LCR* circuit, similar to the dc bias applied. Figure 2(b) shows a significantly better signal-to-noise ratio of $S/N|_1=15$ per field scan in contrast to the conventionally acquired data shown in (a) with $S/N|_1=0.65$ normalized to one scan. The improved signal-to-noise ratio could originate from two effects: (i) at higher probe frequencies in the $1/f$ regime the noise level of the MOSFET is reduced[20] and (ii) the cold amplifier has a better noise performance than the room temperature current amplifier. This high signal-to-noise ratio enables monitoring the device resistance sensitively enough to observe spin-dependent resistance changes by direct acquisition of V_{IF} with DSO. Figure 2(c) shows V_{IF} converted to $I_{\mathrm{SD}}^{\mathrm{IF}}$ using Fig. 1(b) averaged over nine magnetic field scans. Each field point consists of the mean value of V_{IF}, obtained for a 1024-points time trace, where each trace is averaged for 128 times. The ability to directly acquire $I_{\mathrm{SD}}^{\mathrm{IF}}$ in the time domain with a precision that allows to resolve spin-dependent features is the prerequisite for investigating dynamic effects, e.g., resistance changes during or after microwave pulses. In general, the detection bandwidth is limited by the quality factor of the *LCR* circuit, in this case 20 MHz. This would technically allow the direct monitoring of Rabi oscillations, since a typical Rabi frequency in pulsed ESR/EDMR spectrometers is 5–20 MHz (Ref. 9) and should be 2.8 MHz in the devices used in these experiments, based on $B_1=0.1$ mT obtained from numerical modeling.[15]

To experimentally explore the bandwidth of rfEDMR, we investigate the spin-resonant resistance change as function of the microwave frequency modulation rate f_{mod}. Figure 3 compares the conventionally measured (lock-in amplified) peak-to-peak signal amplitudes obtained for the conduction band electron signal at $B_0=1.354\ 29$ T (blue squares) to the data acquired via the reflected rf signal in the tank circuit, again lock-in amplified (solid black circles). While the conventionally detected signal shows a 3 dB compression at $f_{\mathrm{mod}}\approx 15$ kHz, as expected for a device resistance of ≈ 30 kΩ and cable capacitance of $C_{\mathrm{cable}}\approx 400$ pF resulting in a $f_{\mathrm{RC}}\approx 13$ kHz, the $\Delta I_{\mathrm{SD}}^{\mathrm{IF}}$ obtained via the

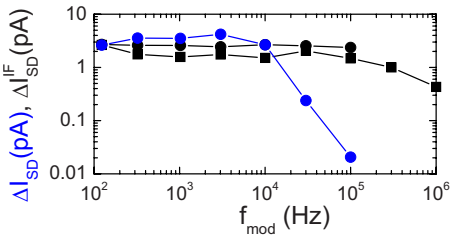

FIG. 3. (Color online) Frequency modulation rate dependence of the signal amplitudes for conventional EDMR and rfEDMR detection. The blue circles represent the peak-to-peak amplitude of the conduction band electron ESR signal using conventional EDMR, decreasing at ≈15 kHz. The rfEDMR lock-in signal (black circles) matches the conventional EDMR data up to $f_{\mathrm{mod}}\approx 15$ kHz and shows no decrease up to 100 kHz. Using a digital storage oscilloscope $I_{\mathrm{SD}}^{\mathrm{IF}}$ was recorded up to $f_{\mathrm{mod}}=1$ MHz and the lock-in response determined numerically (black squares). Here, the signal amplitude starts to drop at about 300 kHz, attributed to the voltage preamplifiers used.

lock-in amplifier shows no frequency dependence up to 100 kHz, the maximum frequency of the SR830 lock-in amplifier. To extend the accessible frequency beyond this limitation, we directly digitized V_{IF} using a DSO and calculated the lock-in signal numerically (solid black circles). For the digital data acquisition we kept the number of recorded modulation periods constant. The response of the *LCR* circuit measured with the SR830 and the "numerical lock-in data" agree quantitatively in the overlapping range, resulting in a measured $f_{3\ \mathrm{dB}}\approx 300$ kHz. This limit is attributed to the SR560 voltage preamplifiers used to postamplify the output of the quadrature demodulation board and could be overcome by higher bandwidth preamplifiers.

In conclusion, we present a high bandwidth detection method to observe EDMR using a *LCR* tank circuit. Measuring rfEDMR for a silicon MOSFET, quantitative agreement with conventionally detected EDMR is demonstrated with a 25-fold increase in the signal-to-noise ratio and a detection bandwidth >300 kHz. These two properties are the key requirement to probe dynamic spin information in the conductance directly, e.g., Rabi oscillations during ESR pulses. Finally, this technique should be sensitive to capacitive changes in the *LCR* circuit as well and might be applicable to capacitive detected magnetic resonance studies.[21]

The authors thank D. Barber for technical support in the National Magnet Laboratory at UNSW. This work is supported by the Australian Research Council, the Australian Government, and by the U.S. National Security Agency (NSA) and U.S. Army Research Office (ARO) (under Contract No. W911NF-04-1-0290).

[1] J.-M. Spaeth and H. Overhof, *Point Defects in Semiconductors and Insulators* (Springer, Berlin, 2003).
[2] A. Schweiger and G. Jeschke, *Principles of Pulse Electron Paramagnetic Resonance* (Oxford University Press, New York, 2001).
[3] D. C. Maier, Bruker Rep. **144**, 13 (1997).
[4] D. R. McCamey, H. Huebl, M. S. Brandt, W. D. Hutchison, J. C. McCallum, R. G. Clark, and A. R. Hamilton, Appl. Phys. Lett. **89**, 182115 (2006).
[5] L. Childress, M. V. Gurudev Dutt, J. M. Taylor, A. S. Zibrov, F. Jelezko, J. Wrachtrup, P. R. Hemmer, and M. D. Lukin, Science **314**, 281 (2006).
[6] F. H. L. Koppens, C. Buizert, K. J. Tielrooij, I. T. Vink, K. C. Nowack, T. Meunier, L. P. Kouwenhoven, and L. M. K. Vandersypen, Nature (London) **442**, 766 (2006).
[7] J. Wrachtrup, C. von Borczyskowski, J. Bernard, M. Orritt, and R. Brown, Nature (London) **363**, 244 (1993).

[8] J. Köhler, J. A. J. M. Disselhorst, M. C. J. M. Donckers, E. J. J. Groenen, J. Schmidt, and W. E. Moerner, Nature (London) **363**, 242 (1993).
[9] A. R. Stegner, C. Boehme, H. Huebl, M. Stutzmann, K. Lips, and M. S. Brandt, Nat. Phys. **2**, 835 (2006).
[10] H. Huebl, F. Hoehne, B. Grolik, A. R. Stegner, M. Stutzmann, and M. S. Brandt, Phys. Rev. Lett. **100**, 177602 (2008).
[11] R. J. Schoelkopf, P. Wahlgren, A. A. Kozhevnikov, P. Delsing, and D. E. Prober, Science **280**, 1238 (1998).
[12] V. Eremin, D. S. Poloskin, E. Verbitskaya, M. P. Vlasenko, L. S. Vlasenko, R. Laiho, and T. O. Niinikoski, J. Appl. Phys. **93**, 9659 (2003).
[13] C. F. O. Graeff, M. S. Brandt, M. Stutzmann, M. Holzmann, G. Abstreiter, and F. Schäffler, Phys. Rev. B **59**, 13242 (1999).
[14] M. Stutzmann, M. S. Brandt, and M. W. Bayerl, J. Non-Cryst. Solids **266**, 1 (2000).
[15] L. H. Willems van Beveren, H. Huebl, D. R. McCamey, T. Duty, A. J. Ferguson, R. G. Clark, and M. S. Brandt, Appl. Phys. Lett. **93**, 072102 (2008).
[16] R. N. Ghosh and R. H. Silsbee, Phys. Rev. B **46**, 12508 (1992).
[17] C. F. Young, E. H. Poindexter, G. J. Gerardi, W. L. Warren, and D. J. Keeble, Phys. Rev. B **55**, 16245 (1997).
[18] P. R. Cullis and J. R. Marko, Phys. Rev. B **11**, 4184 (1975).
[19] G. W. Morley, D. R. McCamey, H. A. Seipel, L.-C. Brunel, J. van Tol, and C. Boehme, Phys. Rev. Lett. **101**, 207602 (2008).
[20] R. Sarpeshkar, T. Delbrück, and C. Mead, IEEE Circuits Devices Mag. **9**, 23 (1993).
[21] M. S. Brandt, R. T. Neuberger, and M. Stutzmann, Appl. Phys. Lett. **76**, 1467 (2000).